PCCP

COMMUNICATION

View Article Online
View Journal | View Issue

Cite this: *Phys. Chem. Chem. Phys.*, 2014, **16**, 21941

Received 9th July 2014,
Accepted 29th August 2014

DOI: 10.1039/c4cp03015j

www.rsc.org/pccp

Solvation structure and energetics of electrolytes for multivalent energy storage†

Saul H. Lapidus,‡[a] Nav Nidhi Rajput,‡[b] Xiaohui Qu,[b] Karena W. Chapman,*[a] Kristin A. Persson*[b] and Peter J. Chupas*[a]

By analysing X-ray pair distribution function data using a multivariate statistical approach, we isolate the cation solvation structure for monovalent (Li^+/Na^+/K^+) and multivalent (Mg^{2+}/Ca^{2+}/Zn^{2+}) electrolytes based on TFSI salts in diglyme. Parallel molecular dynamics simulations provide enhanced structural details. The data suggest that contact ion-pairs are a common feature in multivalent electrolytes.

The pursuit of transformative gains in energy storage capacities is driving innovations in battery chemistries.[1–3] Multivalent batteries, such as those based on divalent Mg^{2+}, Ca^{2+}, Zn^{2+}, or even trivalent Al^{3+} ions, have the potential to provide gains up to 300% in energy storage density, at lower cost and with enhanced safety compared to commercial Li-ion devices.[4–6] However, realising multivalent battery technologies will require developments in both electrode materials and in the electrolytes that facilitate multivalent ion transport and charge transfer.

The choice of electrolyte is critical to battery performance.[7,8] Among many relevant parameters, high ion mobility in the bulk electrolyte and facile (de)solvation of the ion at the electrode interface are required. For example in Li-ion intercalation systems, Li^+ desolvation controls the kinetics of the charge transfer between the bulk electrolyte and the electrode.[1] The challenge in selecting suitable electrolytes is magnified for multivalent batteries. Indeed multivalent (*e.g.* Mg) salts have poor solubility and performance in the best performing Li-ion solvents (*e.g.*, propylene carbonate, ethylene carbonate, ethyl methyl carbonate). The higher charge density of a multivalent ion, compared to Li^+, is likely to contribute to a larger desolvation energy at the electrode interface and a more organised solvation structure that may impede ion mobility.[6,9–11] Fundamental studies of multivalent electrolytes, including the nature and strength of cation interactions with solvent molecules and counter-anions, are critical to the design of new functional electrolytes and, accordingly, multivalent batteries.[5,10,11]

The structure of an electrolyte solution can be evaluated both experimentally and computationally as a pair or radial distribution function (PDF or RDF)—the distribution of distances between pairs of atoms. Experimentally, a PDF can be determined from X-ray total scattering data providing the time-averaged local atomic structure of the electrolyte; peaks in the PDF correspond to distinct atom–atom distances in the system. In molecular modelling, the relative atom positions at a given time can be visualised as a RDF. Accurate simulations require appropriate force fields parameters, which can be selected based on correspondence to experimental PDFs. Conversely, the molecular simulations aid in interpreting experimental data.

Here, we integrate PDF measurements and computational modelling to investigate the structure and energetics of divalent solvation, particularly focusing on the features of Mg^{2+} in a prospective electrolyte for multivalent Mg batteries. While the as-measured PDF includes contributions from all atom–atom pairs—not only between the multivalent cation and solvating molecules but also within and around the counter-anion—we pioneer a new approach, based on principal component analysis (PCA), to analytically isolate the cation solvation environment. This builds on an established differential approach to recover chemically specific insights by subtracting the measured PDF for an isolated component from the total PDF to obtain a differential PDF (*d*-PDF). While the established differential approach relies on being able to isolate and separately probe an individual component, in the case of electrolytes, the critical components (*i.e.* the cation and anion) can never be physically separated. Here, by analysing a series of solutions with the same counter-anion and solvent, the common atom–atom contributions can be analytically identified and subtracted to reveal to the solvation environment of the target cation.

Glyme-based electrolytes have recently demonstrated promising performance characteristics that are of interest for both next-generation Li and multivalent electrolytes.[12–15] For Li systems, glymes show higher conductivity and cycling efficiency

[a] *X-ray Science Division, Advanced Photon Source, Argonne National Laboratory, Argonne, IL, 60439, USA. E-mail: chupas@aps.anl.gov, chapmank@aps.anl.gov*
[b] *Environmental Energy Technology Division, Lawrence Berkeley National Laboratory, Berkeley, CA, 94720, USA. E-mail: KAPersson@lbl.gov*

† Electronic supplementary information (ESI) available. See DOI: 10.1039/c4cp03015j

‡ These authors contributed equally.

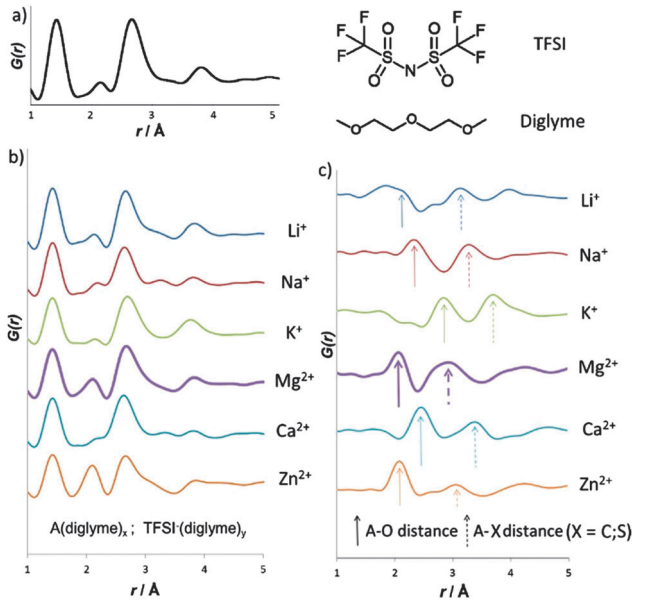

Fig. 1 PDF data for the series of $A(TFSI)_x$–diglyme solutions, A = Li^+, Na^+, K^+, Mg^{2+}, Ca^{2+}, Zn^{2+}, highlighting (a) the common TFSI–TFSI and TFSI–diglyme atom–atom correlations as determined through principal component analysis, (b) the as-measured total PDFs and (c) the *d*-PDFs corresponding to the $A^{+/2+}$ solvation environment. Data have been offset for clarity.

than current leading non-aqueous solvents (*e.g.* EC, MEC).[12,13] For multivalent systems, diglyme solutions of $Mg(TFSI)_2$ (TFSI = bis(trifluoromethanesulfonyl)-imide, see inset Fig. 1) are one of few Mg electrolytes in which reversible electrochemical reactions have been achieved, with evidence of plating/stripping of Mg on a working electrode.[14–16] Accordingly, $Mg(TFSI)_2$–diglyme is an important candidate electrolyte system. In solvents such as glymes with low dielectric constants, pairing of cationic and anionic species can occur in solution. However, the potential for ion-pair formation is likely moderated by both the bulky structure and distributed charge density of the $TFSI^-$ anion, which may decrease the columbic interaction, and the multiple available ether oxygen donors and high donor number of diglyme, which may help solvate the Mg^{2+} cation. The favourable electrochemical performance of $Mg(TFSI)_2$–diglyme suggests that this particular combination of cation–anion–solvent is associated with a solvation structure and energetics that are well suited to multivalent batteries and warrants direct analysis.

X-ray total scattering data for $Mg(TFSI)_2$ (0.4 M in diglyme) were collected at beamline 11-ID-B at the Advanced Photon Source at Argonne National Laboratory.[17,18] Additional data were collected for a series of TFSI–diglyme solutions of different alkali and alkali earth cations (A(TFSI) or $A(TFSI)_2$ for A = Li^+, Na^+, K^+; Ca^{2+}, Zn^{2+}, respectively). The PDFs were derived from the total scattering data, correcting for background (measured for pure diglyme), Compton scattering, and Fourier transforming to $Q_{max} \sim 17.5$ Å^{-1} as described previously.[18]

The as-measured PDFs for TFSI solutions with different cations show a small degree of variability, but are otherwise dominated by common features at ~1.4 Å and ~2.7 Å (Fig. 1b). These shared features, corresponding to atomic distances within TFSI anions and between TFSI···diglyme species, overwhelm the more dilute contributions associated with cation solvation which cannot be straightforwardly resolved.

Using PCA, the common contribution to the PDFs for all electrolyte solutions was evaluated (see ESI†).[19] The principal component includes the intra-molecular atomic distances within individual TFSI anions and inter-molecular TFSI···diglyme atomic distances. The peaks observed at 1.42 Å, 2.68 Å, and 3.81 Å correspond to 1,2-, 1,3- and 1,4- (*i.e.*, O···(SN)···S) distances within TFSI, respectively. A weaker feature at 2.13 Å may be due to a TFSI···diglyme interaction. Due to conformational flexibility and dynamic motion, longer-range features are broadened to the point of being indistinguishable from the background.

Differentials PDFs, which isolate the contribution from the cation solvation structure, were computed based on the analytically-derived reference PDF—the intra-molecular distance dominated principal component. These *d*-PDFs are expected to include features associated with the cation···diglyme and cation···TFSI interactions.

There are significant variations in the *d*-PDFs for the different cations reflecting their distinct cation sizes and solvation structures. Several well-defined narrow peaks are observed at low *r* with broader regularly spaced features at high *r* that appear beyond a threshold distance (in Mg: 0.3–0.6 Å FWHM for low *r*-peaks *cf.* 1.9 Å FWHM for high-*r* peaks). The narrow low *r* peaks correspond to the distances between the cation and the atoms of molecules coordinated in its first solvation shell (see Table 1 and Fig. 2). Interestingly, these well-defined peaks extend to longer distances for the divalent compared to monovalent cations. This observation suggests that the higher charge of the multivalent ion contributes to reduced conformational flexibility and dynamics of the solvating molecules or constrained coordination of larger molecular species. The diffuse high-*r* features correspond to characteristic higher order solvation shells and are generally a consequence of atom packing of a dynamically disordered solvent without any well-defined bonding interactions. These diffuse contributions are most readily visualised in the *r*-weighted form of the PDFs, $rG(r)$, which amplifies longer range features (Fig. 2).

The first peak corresponds to a cation···O distance, which varies for the series as expected based on the cation size ($Li^+ < Na^+ < K^+$, $Mg^{2+} \sim Zn^{2+} < Ca^{2+}$).[20] (Table 1) Specifically, for the Mg–TFSI *d*-PDF, the observed Mg···O distance is 2.08 Å, which is similar to that found in Mg-based solids (*e.g.*, 2.106 Å in rock salt MgO, 2.1–2.3 Å in common Mg silicates)[21] indicates a close, strong interaction. The second peak at 2.94 Å corresponds to

Table 1 Characteristic distances from the *d*-PDFs corresponding to the cation solvation structure

Cation	Cation size[20]/Å	d_{A-O}/Å	d_{A-X}/Å	Higher-order shells/Å	Average shell spacing/Å
Li^+	0.90	2.17	3.13	7.7, 11.8, 15.9	4.1
Na^+	1.16	2.37	3.27	8.2, 12.5, 16.8	4.3
K^+	1.52	2.85	3.66	10.6, 14.6	4.0
Mg^{2+}	0.86	2.08	2.94	9.3, 13.0, 16.8	3.8
Ca^{2+}	1.14	2.45	3.43	11.4, 15.4	3.9
Zn^{2+}	0.88	2.08	3.04	9.2, 13.0	3.8

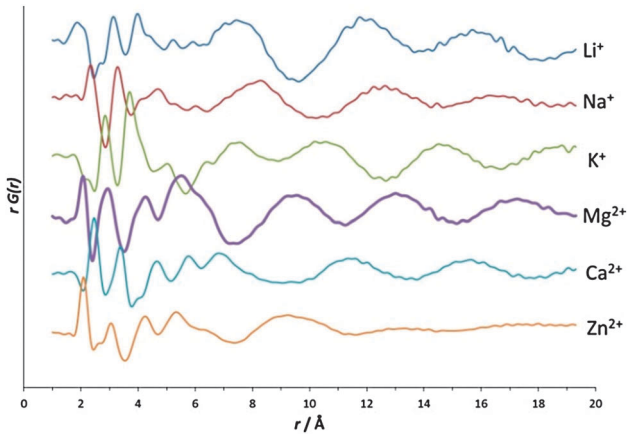

Fig. 2 *r*-Weighted form of the *d*-PDFs, *rG*(*r*), highlights the well-defined inner sphere features and broader solvation shells at longer distances.

the distance between the Mg ion and the atom bonded to the coordinating oxygen. Assuming an O–X bond length of 1.4 Å on average suggests an Mg···O–X angle of *ca.* 115°.

Complementary molecular modelling was independently undertaken for 0.4 M $Mg(TFSI)_2$ in diglyme. The RDFs for selected atom pairs were derived from molecular dynamics (MD) simulations. Simulations were performed within the Gromacs MD package utilising a 40 × 40 × 40 Å box with periodic boundary conditions (see ESI†).[22] Different force field parameters from the literature were evaluated for Mg, TFSI and diglyme and the OPLS-AA parameters provided the best match to the experimental data[23–26] (see ESI†). While generally similar features were found in the RDF from different force fields, small changes in the Mg^{2+} parameters yielded significant changes in the Mg^{2+} coordination; less optimal parameters yielded Mg–O distances that deviated by up to 0.2 Å from the experimental value.[23,27]

The molecular configuration (Fig. 3) suggests that Mg^{2+} is *ca.* 6-fold coordinated by O-donors from diglyme and TFSI

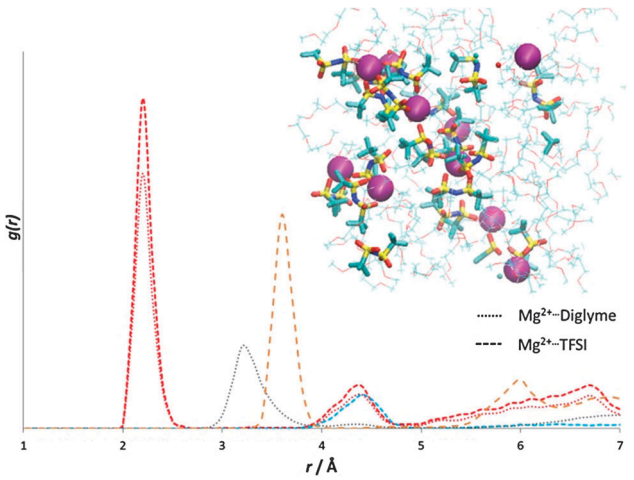

Fig. 3 Atomic-scattering-weighted Mg-X RDFs from MD simulations (O: red, N: blue, C: grey, S: yellow). The corresponding simulation showing Mg^{2+} in space-filling format (magenta), $TFSI^-$ in stick format and diglyme in line format, is inset.

species in the first solvation shell. Both diglyme and TFSI species are largely bidentate, chelated through O-donors, with average coordination numbers of 2.3 and 0.9, respectively. The average Mg···O distance at 2.1 Å that reported for aqueous Mg salts (2.0 Å to 2.12 Å).[28,29] The sharpness of both Mg···O features indicates a strong interaction of the TFSI and diglyme species with the Mg^{2+} cation. For TFSI, the longer Mg···N distance suggests direct N-coordination is hindered by the sulfonyl groups. The MD suggests a predominately linear Mg···O–S configuration which differs from that suggested by the *d*-PDF data or observed in crystalline TFSI salts.[30] This discrepancy in the bond angles and, consequently, in the longer range atomic distances which seem to be systematically offset to higher *r* relative to the experimental data (see Fig. S5, ESI†), may be attributable to the non-polarisable force field parameters used which does not allow redistribution of electron density upon interaction with the cation.

The relatively short Mg···O distances and strong first-shell solvation coordination of both diglyme and TFSI indicate that $Mg(TFSI)_2$–diglyme electrolyte as considerable ion pair and ion triplet interactions. With an average coordination of *ca.* 0.9 TFSI molecules per Mg^{2+} (*ca.* 33% $[Mg(TFSI)_2]_0$, 20% $[Mg(TFSI)]^+$, 47% $[Mg(TFSI)_0]^{2+}$), the ion association not only reduces the effective charge of the solvated cation, but will impact ion mobility and the kinetics/energetics for desolvation of the cation at the electrolyte surface.[31] The persistence of narrow peaks to longer distances in the experimental *d*-PDF for Mg^{2+} can be ascribed to these ion-pairing interactions, with the coordination of larger TFSI anions contributing to longer range peaks than the smaller (with respect to non-H atoms) diglyme. Taking the extended range of narrow features in the *d*-PDFs as a signature of TFSI coordination and ion-pairing, suggests that ion association is a general feature of the multivalent diglyme electrolytes studied here.

Similar Mg–TFSI ion pairs have been documented in ionic liquid electrolytes with electrical conductance studies of other Mg^{2+} solutions suggesting a predisposition towards ion pair formation in weakly coordinating (*i.e.*, low dielectric constant) solvents,[31] although the ultimate solution structure and degree of ion pairing likely varies with counter ion and chelating effects.[23,32] We postulate that the level of ion pairing in diglyme in which favourable electrochemical performance has been demonstrated (an average 0.9 : 1 TFSI : Mg at 0.4 M) may provide a balance between ion mobility and desolvation energies. Longer, more chelating glyme solvents will likely reduce the level of ion pairing at a given concentration.

The desolvation energy is an additional measure of the multivalent ion interactions and can be considered as the energy barrier to detach the cation from its solvent solvation shell. The desolvation energy is also directly related to the charge transfer at the electrode interface[9] and, hence, a critical design metric in the pursuit of novel multivalent electrolytes.[33] Here, the desolvation energy for Mg^{2+} in $Mg(TFSI)_2$–diglyme was computed using a solvent dissociative mechanism and the results are compared with a self-consistent reaction-field implicit solvent model (see ESI†).[34,35] Removing a solvent

molecule from the first Mg^{2+} solvation shell corresponds to an energy barrier of 17.36 kcal mol^{-1}, in qualitative agreement with the desolvation energy of 12.53 kcal mol^{-1} obtained from the SM12-MK implicit solvent model.[35] These values are slightly larger than desolvation energies measured for Li in EC/DMC electrolytes ($\sim$12 kcal mol^{-1}),[9] with the significant difference that Li is well solvated by the solvent molecules in these systems, while the Mg forms ion pairs. Hence, during the electrode interface charge transfer, it is expected that the $Mg(TFSI)_2$–diglyme system will exhibit an additional dissociation penalty correlated with the cohesive energy of the salt.

Conclusions

This work highlights a new approach to derive chemically-specific PDF data that has been applied to gain insight into the solvation structure of multivalent electrolytes. Such fundamental atomic scale understanding of the solvation phenomena for working ions is a critical foundation for the design and development of novel electrolytes for multivalent batteries with high energy density, high safety, and low cost. The analytical approach presented here is broadly applicable to other electrolytes, and only requires a series of systems in which an individual component is systematically varied. The association of Mg^{2+} and $TFSI^-$ in diglyme indicates that the salt is incompletely dissociated with partial compensation of the multivalent cation charge within the adduct. Such ion pairing will be an important consideration when optimising ion mobility in the bulk electrolyte and charge transfer at the electrode interface. The similar solvation structures and length scale of atomic-ordering observed in the *d*-PDFs for the Ca^{2+} and Zn^{2+} systems suggest that such ion pairs are likely a common feature of these other multivalent electrolytes.

Acknowledgements

This work was supported as part of the Joint Center for Energy Storage Research, an Energy Innovation Hub funded by the U.S. Department of Energy, Office of Science, Basic Energy Sciences. Work done at Argonne and use of the Advanced Photon Source, and Office of Science User Facility operated for the U.S. Department of Energy Office of Science by Argonne National Laboratory, were supported by the U.S. Department of Energy under Contract No. DE-AC02-06CH11357. Work at Lawrence Berkeley National Laboratory was supported by the Assistant Secretary for Energy Efficiency and Renewable Energy, under Contract No. DEAC02-05CH11231. We thank the National Energy Research Scientific Computing Center (NERSC) for computing resources and Bachir Aoun for discussions.

Notes and references

1 P. Albertus, G. Girishkumar, B. McCloskey, R. S. Sánchez-Carrera, B. Kozinsky, J. Christensen and A. Luntz, *J. Electrochem. Soc.*, 2011, **158**, A343–A351.
2 B. D. McCloskey, R. Scheffler, A. Speidel, D. S. Bethune, R. M. Shelby and A. C. Luntz, *J. Am. Chem. Soc.*, 2011, **133**, 18038–18041.
3 D. Aurbach, Z. Lu, A. Schechter, Y. Gofer, H. Gizbar, R. Turgeman, Y. Cohen, M. Moshkovich and E. Levi, *Nature*, 2000, **407**, 724–727.
4 D. Aurbach, I. Weissman, Y. Gofer and E. Levi, *Chem. Rec.*, 2003, **3**, 61–73.
5 H. S. Kim, T. S. Arthur, G. D. Allred, J. Zajicek, J. G. Newman, A. E. Rodnyansky, A. G. Oliver, W. C. Boggess and J. Muldoon, *Nat. Commun.*, 2011, **2**, 427.
6 R. E. Doe, R. Han, J. Hwang, A. J. Gmitter, I. Shterenberg, H. D. Yoo, N. Pour and D. Aurbach, *Chem. Commun.*, 2014, **50**, 243–245.
7 T. R. Jow, K. Xu, O. Borodin and M. Ue, *Electrolytes for Lithium and Lithium-Ion Batteries*, Springer, 2014.
8 M. Park, X. Zhang, M. Chung, G. B. Less and A. M. Sastry, *J. Power Sources*, 2010, **195**, 7904–7929.
9 K. Xu and A. von Wald Cresce, *J. Mater. Res.*, 2012, **27**, 2327–2341.
10 Q. Zhao, Y. NuLi, T. Nasiman, J. Yang and J. Wang, *Int. J. Electrochem. Sci.*, 2012, **2012**, 701741.
11 P. Wang, Y. NuLi, J. Yang and Z. Feng, *Surf. Coat. Technol.*, 2006, **201**, 3783–3787.
12 S. Tobishima, H. Morimoto, M. Aoki, Y. Saito, T. Inose, T. Fukumoto and T. Kuryu, *Electrochim. Acta*, 2004, **49**, 979–987.
13 I. Geoffroy, P. Willmann, K. Mesfar, B. Carré and D. Lemordant, *Electrochim. Acta*, 2000, **45**, 2019–2027.
14 Y. Shao, M. Gu, X. Li, Z. Nie, P. Zuo, G. Li, T. Liu, J. Xiao, Y. Cheng, C. Wang, J.-G. Zhang and J. Liu, *Nano Lett.*, 2013, **14**, 255–260.
15 S.-Y. Ha, Y.-W. Lee, S. W. Woo, B. Koo, J.-S. Kim, J. Cho, K. T. Lee and N.-S. Choi, *ACS Appl. Mater. Interfaces*, 2014, **6**, 4063–4073.
16 T. T. Tran, W. M. Lamanna and M. N. Obrovac, *J. Electrochem. Soc.*, 2012, **159**, A2005–A2009.
17 P. J. Chupas, K. W. Chapman and P. L. Lee, *J. Appl. Crystallogr.*, 2007, **40**, 463–470.
18 P. J. Chupas, X. Qiu, J. C. Hanson, P. L. Lee, C. P. Grey and S. J. L. Billinge, *J. Appl. Crystallogr.*, 2003, **36**, 1342–1347.
19 S. H. Lapidus, P. J. Chupas and K. W. Chapman, *J. Appl. Crystallogr.*, 2014, submitted.
20 R. Shannon, *Acta Crystallogr., Sect. A: Fundam. Crystallogr.*, 1976, **32**, 751–767.
21 *Crystallographic Databases*, ed. G. Bergerhoff and I. D. Brown, International Union of Crystallography, (Hrsg.) Chester, 1987.
22 S. Pronk, S. Páll, R. Schulz, P. Larsson, P. Bjelkmar, R. Apostolov, M. R. Shirts, J. C. Smith, P. M. Kasson and D. van der Spoel, *Bioinformatics*, 2013, **29**, 845–854.
23 K. M. Callahan, N. N. Casillas-Ituarte, M. Roeselová, H. C. Allen and D. J. Tobias, *J. Phys. Chem. A*, 2010, **114**, 5141–5148.
24 M. S. Cates, M. L. Teodoro and G. N. Phillips Jr, *Biophys. J.*, 2002, **82**, 1133–1146.
25 W. L. Jorgensen, *OPLS and OPLS-AA Parameters for Organic Molecules, Ions, and Nucleic Acids*, New Haven, CT, 1997.

26 M. S. Kelkar and E. J. Maginn, *J. Phys. Chem. B*, 2007, **111**, 4867–4876.
27 J. Aaqvist, *J. Phys. Chem.*, 1990, **94**, 8021–8024.
28 G. I. Szász, W. Dietz, K. Heinzinger, G. Pálinkas and T. Radnai, *Chem. Phys. Lett.*, 1982, **92**, 388–392.
29 B. Minofar, R. Vácha, A. Wahab, S. Mahiuddin, W. Kunz and P. Jungwirth, *J. Phys. Chem. B*, 2006, **110**, 15939–15944.
30 L. Xue, D. D. DesMarteau and W. T. Pennington, *Solid State Sci.*, 2005, **7**, 311–318.
31 A. Apelblat, *J. Solution Chem.*, 2011, **40**, 1234–1257.
32 A. Wahab, S. Mahiuddin, G. Hefter, W. Kunz, B. Minofar and P. Jungwirth, *J. Phys. Chem. B*, 2005, **109**, 24108–24120.
33 K. Xu, A. von Cresce and U. Lee, *Langmuir*, 2010, **26**, 11538–11543.
34 Y. Yang, N. Sahai, C. S. Romanek and S. Chakraborty, *Geochim. Cosmochim. Acta*, 2012, **88**, 77–87.
35 A. V. Marenich, C. J. Cramer and D. G. Truhlar, *J. Chem. Theory Comput.*, 2012, **9**, 609–620.